Journal of Building Engineering 8 (2016) 243–248

Contents lists available at ScienceDirect

Journal of Building Engineering

journal homepage: www.elsevier.com/locate/jobe

Saltwater experiments with air curtains for smoke control in the event of fire

J.C. Viegas

Laboratório Nacional de Engenharia Civil, Av. do Brasil 101, 1700-066 Lisboa, Portugal

ARTICLE INFO

Keywords:
Fire safety
Smoke control
Plane jets
Experiments
Saltwater modelling

ABSTRACT

Smoke flow inside buildings is a major cause of death in the event of fire. Presently, fire or smoke doors are used, together with smoke control systems, to avoid smoke flowing beyond the boundaries of the fire compartment. In this research, it is proposed the use of downward air curtains to stop smoke flow, which will not impair visibility in escape routes. The methodology followed in this research includes: (i) the development of an analytical model that relates the relevant characteristic quantities of a plane jet with the characteristics of the environment in which the fire develops, (ii) small scale experiments with saltwater modelling to assess the convective parameters that control the smoke tightness of the curtain, (iii) CFD simulations to assess the performance of a full scale air curtain near a fire source and (iv) fire experiments with a full-scale test specimen. In this paper both the analytical model and the saltwater experiments are presented. Test results confirm that vertical downward air curtains are able to avoid smoke flow through openings and show a good agreement with the theoretical model for predicting the minimum exhaust rate from the fire compartment. It has been shown that the exhaust flow rate depends on the air curtain flow rate and on the fluid heat expansion due to fire. Test results also make it possible to assess the minimum nozzle velocity to avoid smoke leakage.

1. Introduction

Smoke flow inside buildings is a major cause of fire casualties. The technology currently used to prevent these fatalities relies on the enclosure of building spaces by fire resistant walls, on the use of fire resistant doors and on the use of smoke control systems. In many cases, closing passageways with fire doors makes it difficult to identify the escape route and can delay people's egress; in other cases, the use of fire gates makes it difficult to use them as escape routes. When the fire propagation through the void is unlikely, it is acceptable to use an air curtain if effective for stopping the smoke flow. Air curtains do not impair the visibility of building occupants in evacuation and do not pose difficulties to people using escape routes.

There are several applications of this concept in tunnels [1] and in building corridors [2], but these are based on the pull-push principle applied to horizontal air curtains. Several authors have studied the application of single vertical air curtains (upward or downward) [3–8] and a research work has been done about double vertical air curtains [9,12,16]. Some studies used CFD simulations to assess the performance of air curtains as regards curtain tightness in corridors [8], fire/explosion accidents in a clean room [10], contaminant dispersion from clean rooms [11] and as regards curtain tightness in staircases [17].

The mentioned research work is not presenting clearly the need for smoke exhaustion in the fire compartment, which the author of this paper considers it to be a key issue for achieving smoke tightness by air curtains for high temperature smoke. Therefore, further research must be done on this topic in order to obtain a more generalized application of air curtains to the open boundaries of fire compartments.

This project aims to develop and apply air curtain technology to limit smoke flow through the building openings. The methodology followed in this research includes: (i) the development of an analytical model that relates the relevant characteristic quantities of a plane jet with the characteristics of the environment in which the fire occurs, (ii) small scale experiments with saltwater modelling to assess the convective parameters that control smoke tightness of the curtain, (iii) CFD simulations to assess the performance of a full scale air curtain near a fire source and (iv) fire experiments with a full-scale test specimen. This paper addresses both the analytical model and the saltwater experiments.

The analytical model assumes that the pressure due to the jet momentum balances the pressure due to buoyancy at the opening. This model also includes a simplified analytical methodology for estimating the temperature inside the fire compartment.

Several vertical downward plane jets, vertical upward plane jets and

E-mail address: jviegas@lnec.pt.

http://dx.doi.org/10.1016/j.jobe.2016.08.008
Received 9 January 2016; Received in revised form 14 June 2016; Accepted 9 August 2016
Available online 04 October 2016
2352-7102/

horizontal plane jets were tested on a small-scale model (1/20). However, just the vertical downward plane jets proved to be more efficient; therefore, only these results will be reported in this paper. Buoyancy due to fire was reproduced by the difference in density between saltwater and freshwater. The model, made by Plexiglas, includes one compartment connected to the exterior by a single opening, which is protected by the plane jet. The similarity laws between flows enable the extrapolation of these results to real fire cases.

The results showed that it is feasible to avoid the leakage of the denser fluid (simulating smoke) to the exterior of the compartment using a plane jet (curtain) flowing a less dense fluid. The tests clearly showed that the plane jet is critical to the tightness because when it is stopped (with no change in other relevant parameters, including the exhaust flow rate and the intensity of the saltwater source) the loss of tightness occurs immediately. Thus, the test results demonstrate the feasibility of using air curtains to control smoke and enable the experimental assessment of the parameters that control tightness.

2. Methods

2.1. Analytical model

Smoke tightness due to an air curtain (plane jet) is based on the balance of the air curtain momentum and on the momentum of the smoke flow. The nozzle of the plane jet is put at door soffit level and flows downward, $\propto_0$ being the angle between the curtain axis and the vertical plane. The initial momentum J_0 jet per unit of width (of the opening) is given by Eq. (1).

$$J_0=\rho b_0 u_0^2 \tag{1}$$

where ρ is the fluid density, b_0 the thickness of the jet nozzle and u_0 the initial jet velocity. This work considers that the jet momentum is maintained. Since the smoke flow (horizontal, in this case) is normal to the plane of the opening (vertical), only the momentum due to the horizontal component of the jet velocity is concerned, according to Eq. (2). The effect of this momentum (per unit width of the jet) on pressure is assessed by Eq. (3), where h is the vertical height above which the horizontal component of the velocity of the jet comes to zero (i.e. wherein the jet bends to the vertical). The difference in fluid density between indoors and outdoors, assuming a uniform density in each environment, the value of the pressure difference is given by Eq. (4), H being the height above the neutral plane (when the difference in densities is uniform, the pressure difference varies linearly with height).

$$J_{0h}=\rho b_0 u_0^2 \sin\propto_0 \tag{2}$$

$$\Delta P_a=\frac{\rho_0 b_0 u_0^2 \sin\propto_0}{h} \tag{3}$$

$$\Delta P_s=gH(\rho_0-\rho_1) \tag{4}$$

Since the effect of the jet is relevant above the neutral plane only, when the internal pressure is higher than the external pressure, then, h in Eq. (3) is the height of the opening soffit above the neutral plane. The maximum pressure difference occurs near the soffit of the opening. Dividing Eq. (3) by Eq. (4) the pressure ratio obtained is a measure of the performance of the curtain, as Eq. (5) shows. Eq. (6) defines the deflection modulus D_m [12], which is proportional to Eq. (5).

$$\frac{\Delta P_a}{\Delta P_s}=\frac{\rho_0 b_0 u_0^2 \sin\propto_0}{gh^2(\rho_0-\rho_1)} \tag{5}$$

$$D_m=\frac{\rho_0 b_0 u_0^2}{gh^2(\rho_0-\rho_1)} \tag{6}$$

Smoke tightness is obtained by combining the jet momentum with the inlet velocity through the opening due to smoke exhaustion in the compartment. The inflow velocity u_a through the opening contributes also to retain smoke; therefore, its momentum must be considered and Eq. (3) is modified as presented in Eq. (7). Then, Eq. (5) takes the form of Eq. (8).

$$\Delta P_a=\frac{\rho_0 b_0 u_0^2 \sin\propto_0 + \rho_0 h u_a^2}{h} \tag{7}$$

$$\frac{\Delta P_a}{\Delta P_s}=\frac{\rho_0 b_0 u_0^2 \sin\propto_0 + \rho_0 h u_a^2}{gh^2(\rho_0-\rho_1)} \tag{8}$$

The minimum ratio $\Delta P_a/\Delta P_s$=B was assessed by saltwater experiments. Knowing this value, the minimum jet velocity that complies with the smoke tightness requirement is given by Eq. (9). The difference in densities can be obtained from the ideal gas equation and may be expressed in terms of indoor and outdoor temperatures, considering Eq. (10). Combining Eqs. (9) and (10), Eq. (11) is obtained.

$$u_0=\sqrt{\frac{Bgh^2(\rho_0-\rho_1)-\rho_0 h u_a^2}{\rho_0 b_0 \sin\propto_0}} \tag{9}$$

$$\rho_0\frac{T_0}{T_1}=\rho_1 \tag{10}$$

$$u_0=\sqrt{\frac{Bgh^2\left(1-\frac{T_0}{T_1}\right)-hu_a^2}{b_0 \sin\propto_0}} \tag{11}$$

Another part of the problem is to estimate the exhaust flow rate of the smoke control system of the compartment to keep the smoke tightness of the door. As will be shown, it is impossible to obtain smoke tightness of the door without exhausting smoke from the compartment. It is well known that it is possible to obtain smoke tightness of the door if the exhaust rate is high enough; the advantage of using the air curtain is to reduce significantly the exhaust flow rate needed to avoid smoke leakage through the door. Having this in view, the problem of using air curtains to keep the opening tight will be solved if the jet velocity u_0 and the exhaust flow rate are determined as a function of the fire scenario. From Eq. (11) the assessment of u_0 will be solved, if B is known. In this step, it is necessary to assess the exhaust flow rate.

For a compartment with a fire source and an external opening it is clear that to prevent smoke from flowing through this opening to the exterior, the following aspects must be taken into account: (i) the thermal expansion of the smoke into the compartment and (ii) the outer flow entrained by the plane jet at the door. It is also clear that eddies due to jet turbulence near the door may transport to the exterior smoke mixed with the jet flow. In this stage of the work, it will be considered that eddy smoke transport will be prevented by increasing the estimation of the outer flow entrained by plane jet at the door.

The thermal expansion of fluid $\Delta\dot{V}=\dot{V}_1-\dot{V}_0$ (indices 0 and 1 represent the initial and final states, respectively), due to the convective part of the heat release rate, $\dot{Q}_c$, can be estimated by taking into account that the thermal energy conservation can be simplified to Eq. (12), where $\dot{M}$ is the mass flow rate of the fluid, $\overline{C_p}$ the average specific heat at constant pressure (considering here that the average is an approach, which does not have significant consequences since the final equations will be adjusted by empirical coefficients), T_1 the absolute temperature of the hot fluid and T_0 the initial temperature. Using Eq. (10), Eq. (12) can be rewritten as Eq. (13). Eq. (14) refers to the thermal expansion. The flow rate $\dot{V}$ of the plane jet is given by Eq. (15) [13], where x is the distance from the nozzle, b_0 the thickness of the nozzle, w the width of the nozzle (and door) and $\dot{V}_0$ the jet flow rate at the nozzle.

$$\dot{Q}_c=\dot{M}\overline{C_p}(T_1-T_0) \tag{12}$$

$$\dot{Q}_c = \dot{V}_0 \rho_0 \overline{C_p} \left(\frac{\rho_0}{\rho_l} - 1 \right) T_0 \tag{13}$$

$$\frac{\dot{Q}_c}{\rho_0 \overline{C_p} T_0} = \dot{V}_0 \left(\frac{\rho_0}{\rho_l} - 1 \right) = \dot{V}_l - \dot{V}_0 = \Delta \dot{V} \tag{14}$$

$$\dot{V} = 0,44 \left(\frac{x}{b_0} \right)^{0,5} \dot{V}_0 = 0,44 (b_0 x)^{0,5} u_0 w \tag{15}$$

The minimum exhaust flow rate of smoke from the compartment will be the sum of the corresponding thermal expansion with at least the entrained flow of the jet from the exterior. The jet entrains fluid from both sides, but just the flow rate coming from the exterior and the flow rate at the nozzle correspond to the mass intake into the compartment. We must keep in mind that turbulent transport in the jet may require a higher flow rate to maintain smoke tightness. Thus, the minimum exhaust flow rate $\dot{V}_{exaust}$ includes the thermal expansion and a portion proportional to the jet flow rate, according to Eq. (16), A being a constant of proportionality, which includes the geometry of the opening, to be assessed by experiments.

$$\dot{V}_{exaust} = \frac{\dot{Q}_c}{\rho_0 \overline{C_p} T_0} + A b_0^{0,5} u_0 \tag{16}$$

In order to fully solve Eq. (11), it is necessary to estimate the smoke temperature T_l and h. This temperature depends on the convective part of the heat release rate $\dot{Q}_c$ (it is assumed here that in the initial stage of the fire most of the radiated energy is being absorbed by the envelope, and does not contribute to heating of the smoke) and on the exhaust flow rate. Eq. (12) is used to estimate the average temperature of the smoke, but now considering the values of the specific heat at constant pressure, which correspond to the initial and final temperatures (C_{p0} and C_{p1}), as shown in Eq. (17).

$$\dot{Q}_c = \dot{M} (C_{p1} T_l - C_{p0} T_0) \tag{17}$$

Since the exhaust fans keep the flow rate volume approximately constant, it is convenient to express Eq. (17) as a function of volume flow rate of the fan, as shown in Eqs. (18) and (19). The final temperature is then calculated according to Eq. (20). The final temperature dependence on C_{p1} requires an iterative solution.

$$\dot{Q}_c = \rho_0 T_0 \dot{V}_{exaust} \left(C_{p1} - C_{p0} \frac{T_0}{T_l} \right) \tag{18}$$

$$C_{p0} \frac{T_0}{T_l} = C_{p1} - \frac{\dot{Q}_c}{\rho_0 T_0 \dot{V}_{exaust}} \tag{19}$$

$$T_l = \frac{C_{p0} T_0}{C_{p1} - \frac{\dot{Q}_c}{\rho_0 T_0 \dot{V}_{exaust}}} \tag{20}$$

There are a number of methods that allow estimating the position of the neutral plane (e.g., see [14]). The results of the experiments show that the flow near the jet is quite complex and that the neutral plane may be strongly disturbed. Therefore, further results will be referenced to the height of the opening.

2.2. Saltwater modelling

In fire scenarios the flow is buoyancy driven. Using saltwater and freshwater is a good way to scale the difference in density that occurs between smoke and cold air. In this approach, only the convection is retained; it does not make it possible to reproduce radiation heat transfer or chemical reactions. Therefore, just the phenomena related with the flow driven by the air curtain near the opening are studied. This enables some simplification of experiments, in particular: (i) the saltwater (simulating smoke) feeds directly the smoke layer (this avoids plume flow, which is irrelevant for the jet flow, and has the advantage of the saltwater layer density being easier to control); and (ii) the velocity through the opening is created by exhaustion in the fresh water layer (hence the total mass of saltwater needed for experiments is much lower). To reduce the problem of smoke control only to the convective part is an approximation that is reasonable in an initial fire stage, when the cold air flow rate is high and the heat release rate of the heat source is still relatively low, thus corresponding to many smoke control scenarios.

Table 1
Dimensionless variables for fire similarity with saltwater [15].

Dimensionless variable	Definition	
	Prototype	Model
θ^*	$\frac{(T - T_0)}{T_0 \zeta}$	$\frac{Y}{\zeta}$
ζ	U^2/gH	U^2/gh
t^*	$\frac{t_g U}{H}$	$\frac{t_s U}{h}$
$\overline{u}^*$	$\frac{\overline{u}}{U}$	$\frac{\overline{u}}{U}$
$\overline{p}^*$	$\overline{p}/\rho_0 U^2$	$\overline{p}/\rho_0 U^2$
∇^*	$H\nabla$	$h\nabla$
$\overline{x}^*$	$\overline{x}_g/H$	$\overline{x}_s/h$
P =Pr = Sc	$\frac{\mu c_p}{k}$	$\frac{\mu}{\rho_0}\mathfrak{D}$
U	$\left(\frac{\dot{Q}_0 g}{\rho_0 c_p T_0 H}\right)^{1/3}$	$\left(\frac{\dot{m}_0 g}{\rho_0 h}\right)^{1/3}$
Re	$\rho_0 UH/\mu$	$\rho_0 Uh/\mu$
G	$(H/L)^3$	$(h/l)^3$
Q*	$\dot{Q}'''/\left(\frac{\dot{Q}_0}{L^3}\right)$	$\dot{m}'''/\left(\frac{\dot{m}_0}{l^3}\right)$

Saltwater similarity is a good means to generate buoyancy and this is generally achieved using a source of saltwater (coloured for visualization) to simulate the convective plume in a freshwater environment. The saltwater having a greater density than freshwater, the plume is downward generated, leading the similarity to be interpreted upside down. However, except for such minor nuisance, this concept of similarity makes it possible to minimize salt consumption.

The equations of continuity (21), momentum transport (22) and energy conservation (in the form of transport equation) (23) are shown below [15]. Table 1 presents the similarity between the dimensionless variables in the prototype and in the model.

$$\frac{D\overline{u}^*}{Dt^*} = 0 \tag{21}$$

$$\frac{D\overline{u}^*}{Dt^*} + \nabla^* \overline{p}^* - \theta^* \overline{k} = \left(\frac{1}{Re} \right) \nabla^{*2} \overline{u}^* \tag{22}$$

$$\frac{D\theta^*}{Dt^*} = GQ^* + \left(\frac{1}{Re\ Pr^*} \right) \nabla^{*2} \theta^* \tag{23}$$

In the equations above and in Table 1, H and L represent the enclosure height of the prototype and the diameter of the fire in the prototype, respectively. U is the velocity scale of the fluid, ζ the density (or temperature) perturbation scale, Q_0, u, ρ_0, T_0, g, μ, k and c_p respectively represent the convective heat release rate, the velocity, the cold fluid density, the initial temperature, the acceleration of gravity, the viscosity, the thermal conductivity and the specific heat at constant pressure of the air at point $\overline{x}_g$ and time t_g, in the prototype, or time t_s and point $\overline{x}_s$ in the model. The variables applied to the saltwater model are h and l, representing respectively the height and diameter of the saltwater source. Y is the mass fraction of salt, $\mathfrak{D}$ the mass diffusivity, $\dot{m}_0$ the mass flow of salt at the source and Re, Pr and Sc, respectively represent the Numbers of Reynolds, Prandtl and Schmidt.

To ensure a similarity between flows, these must be fully turbulent at the source and, simultaneously, the momentum of the source must be small when compared to the buoyancy (heat source momentum at the origin is zero). According to [15], to satisfy this condition, ratio F (24) must always be less than 1 at the plume, except near the source (u_0 being the velocity at the source and z the height). According to [15], it is reasonable that $F < 1$ for $z > 0.2$ H.

The relationship between buoyancy in the saltwater model and the temperature difference in the prototype can be estimated according to (25) (Froude Number similarity). Subscripts m and P stand for model and prototype, respectively. To obtain a full dynamic similarity the flows must have the same turbulent behaviour.

$$F = \rho u_0/2(\rho - \rho_0)gz \tag{24}$$

$$\frac{u_m}{u_P}=\frac{\sqrt{2gl_m(\rho-\rho_0)_m/\rho_m}}{\sqrt{2gl_P(\rho-\rho_0)_P/\rho_P}} \Longleftrightarrow (T-T_0)_P=\frac{L}{l}\left[1-\left(\frac{\rho_0}{\rho}\right)_m\right]T_{0P} \tag{25}$$

2.3. Saltwater experiments

The saltwater experiments have been carried out inside a glass tank 0.55 m high, 1.40 m long and 0.45 m wide. A Plexiglas model, 0.250 m high, 0.400 m long and 0.250 m wide, was placed 100 mm above the tank bottom (Fig. 1). It had a vertical opening of 0.125 m×0.125 m, with the sill at bottom level of the model. The smoke was simulated by a saltwater in a freshwater environment. The model was placed inside the tank upside down. The saltwater was coloured to allow observation. This model represented a compartment in the geometrical scale 1/20..

The saltwater was pumped directly into the saltwater layer at a flow rate of 0.0427 l/s (the estimated uncertainty corresponded to 1% of the flow rate). The downward plane jet was located outside the model and was fed with freshwater (taken from the tank). Compartment exhaust was achieved at the bottom (top, on the upside down model) of the vertical wall opposite to the opening. Freshwater was constantly fed to the tank in order to maintain the water level. The testing parameters are shown in Table 2. The flow parameters were measured at a steady state before testing or, whenever relevant, they were adjusted (one at a time) during the test to achieve smoke tightness at the opening. The jet angle (with the vertical plane) and the nozzle thickness were varied (at a time) for each jet configuration. In each test, the parameters of jet velocity and exhaust flow rate were adjusted until no saltwater leakage was visible (Fig. 1). The flow rate was determined by calibration of the respective valve position.

The estimated expanded uncertainty corresponded to $U(\rho)=\pm 1.16 \text{kg/m}^3$, for density measurement, $U(b_0)=\pm 0.00002$m, for jet thickness measurement, $U(\propto_0)=\pm 0.05^{\circ}$, for jet angle measurement, $U(u_0)=\pm 0.016$m/s, for jet velocity measurement and to 1% of the inflow velocity u_a. The coverage factor was k=2.

The no smoke (coloured saltwater) leakage threshold was assessed visually through the opening and recorded on video. The most significant component of the uncertainty of the experiments is the visual assessment of the saltwater tightness.

3. Analysis of the experiments

Test results were used to calculate $\Delta P_a/\Delta P_s$, according to Eq. (8). Theoretically, the salt water tightness at the opening is reached when $\Delta P_a/\Delta P_s=1$. Other variables were expected to influence the tightness threshold during the experiments. The results were found to depend only on the calculated average opening velocity (u_a), on the jet velocity (u_0), on the sin of the jet angle ($\sin\propto_0$), on the density difference ($\rho_0-\rho_1$) and on the nozzle thickness (b_0); a new equation being set, of which the parameters were adjusted by the least square method (see Eq. (26)). The exponents were rounded to the nearest fraction and, then, Eq. (26) was simplified to Eq. (27), coefficient 6125 being found when using again the least squares method. Fig. 2 presents the experimental results according to Eq. (28), which shows a good linear correlation. It was observed that this set of data is not related with buoyancy.

$$\frac{\Delta P_a}{\Delta P_s}=\frac{\rho_0 b_0 u_0^2 \sin\propto_0 + \rho_0 h u_a^2}{gh^2(\rho_0-\rho_1)}=5523u_a^{0.702}u_0^{1.261}b_0^{0.637}(\sin\propto_0)^{0.679}\frac{1}{(\rho_0-\rho_1)} \tag{26}$$

$$\frac{\rho_0 b_0 u_0^2 \sin\propto_0 + \rho_0 h u_a^2}{gh^2(\rho_0-\rho_1)}=6125u_a^{2/3}u_0^{4/3}b_0^{2/3}(\sin\propto_0)^{2/3}\frac{1}{(\rho_0-\rho_1)} \tag{27}$$

$$\frac{\rho_0 b_0 u_0^2 \sin\propto_0 + \rho_0 h u_a^2}{gh^2 u_0^{4/3} b_0^{2/3}(\sin\propto_0)^{2/3}}=6125u_a^{2/3} \tag{28}$$

.

Solving Eq. (28) it is possible to obtain the value of the inlet velocity u_a, as shown in Eq. (29), A^* being a constant depending on the initial conditions and geometry of the problem. For these experiments, value A^* varied between 0.36 and 0.44, 0.39 being the average and 0.02 the standard deviation. This value represents the entrainment of flow by the plane jet and theoretically the value of this coefficient is 0.44 [13]. In this case, the experimental average was obtained considering the 20 experimental results available. Even taking into account the experimental dispersion, these results point to a coefficient lower than the theoretical value of 0.44. It is now clear that this test result corresponds to Eq. (15), which was obtained with theoretical considerations; therefore, Eq. (30) will replace Eq. (15) in the mathematical model.

$$u_a=A^* u_0 b_0^{0.5}/h^{0.5}=0.\ 39u_0 b_0^{0.5}/h^{0.5} \tag{29}$$

$$\dot{V}=u_a hw = A^* u_0(b_0 h)^{0.5}w = Ab_0^{0,5}u_0 \tag{30}$$

Only in tests 22–25 the jet velocity was set to a minimum. In all the other cases, the jet velocity was higher; therefore, the saltwater tightness at the opening was conditioned by jet turbulence and by jet entrained flow rate from the exterior, which will be balanced by the exhaust flow rate. That is why Eq. (28) does not depend on buoyancy. Only the results of tests 22–25 will be directly related with buoyancy; thus, these results may be used in Eq. (8) to obtain the tightness condition related to buoyancy, as shown in Eq. (31), in which Eq. (29) was included. The ratio $\Delta P_a/\Delta P_s$ varies from 0.0071 (in test 23) to 0.0301 (in test 24), the average being 0.0195. These values correspond

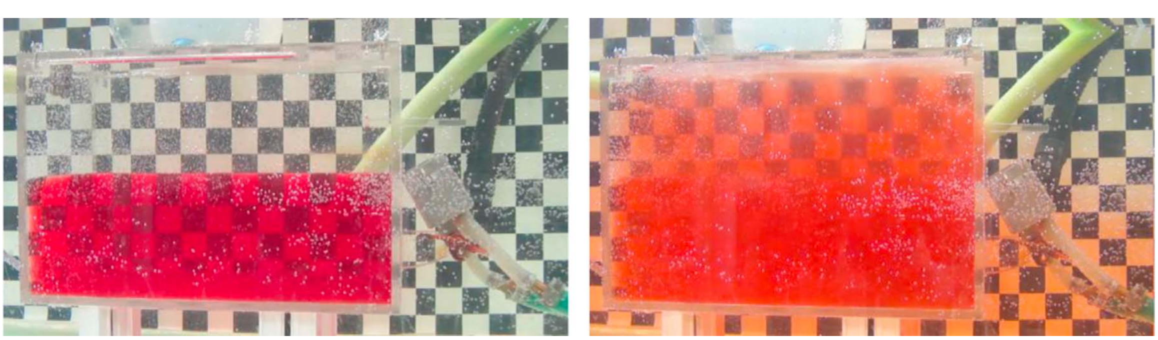

Fig. 1. Saltwater model before testing (left) and during test (right), showing saltwater tightness.

Table 2
Saltwater test parameters.

Test number	b_0 [m]	u_0 [m/s]	$\propto_0$ [deg.]	Initial ρ_0 [kg/m³]	Final ρ_0 [kg/m³]	ρ_1 [kg/m³]	u_a [m/s]
1	0.00250	0.560	25	970.0	970.0	1023.4	0.0394
2	0.00500	0.560	25	968.7	968.7	1026.3	0.0508
3	0.00125	0.560	25	968.6	968.6	1027.8	0.0337
4	0.00750	0.458	25	976.4	976.4	1033.9	0.0436
5	0.00750	0.458	25	964.2	974.7	1020.1	0.0561
6	0.00125	0.700	25	968.1	975.4	1025.9	0.0289
7	0.00125	0.850	25	960.2	977.3	1024.4	0.0371
8	0.00125	1.000	25	963.2	973.3	1028.0	0.0376
9	0.00125	1.000	30	965.5	978.9	1026.9	0.0382
10	0.00125	0.850	30	973.0	975.5	1025.5	0.0384
11	0.00125	0.700	30	969.8	977.9	1026.7	0.0325
12	0.00125	0.560	30	969.8	974.8	1026.7	0.0310
13	0.00125	0.560	35	972.4	972.6	1031.7	0.0467
14	0.00125	0.700	35	975.8	979.6	1026.2	0.0462
15	0.00125	0.850	35	955.3	956.0	1019.0	0.0403
16	0.00125	1.000	35	955.3	956.9	1019.0	0.0559
22	0.00125	0.401	30	965.4	967.9	1032.1	0.0269
23	0.00125	0.142	30	975.6	979.1	1003.0	0.0113
24	0.00125	0.456	30	973.9	979.6	1012.7	0.0178
25	0.00125	0.321	30	968.1	970.7	1003.2	0.0209

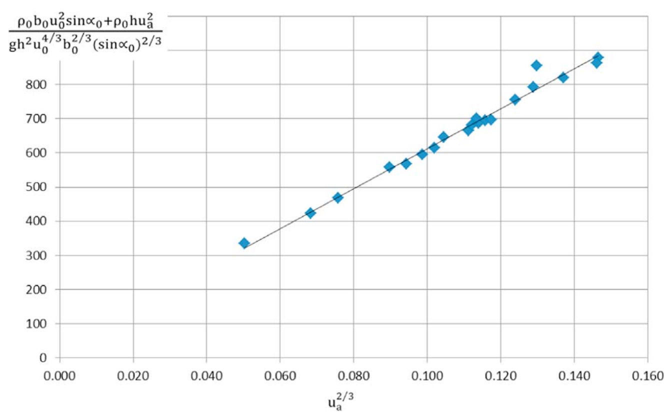

Fig. 2. Best fit of experimental results, by linear relation.

to the four extreme left points in the graph of the Fig. 2. Just the lowest one (0.0017 in test 23) correspond to the optimal condition (extreme left point of the graph of the Fig. 2), because physically correspond to the test with the lowest momentum in the plane jet where was still possible to keep the salt water (representing the smoke) inside the compartment. As a consequence, the exhaust flow rate is also the lowest obtained in the tests; this is the purpose of this technology. However, it seems to be wise to consider a more conservative value of the ratio $\Delta P_a/\Delta P_s$ in order that the salt water tightness at the door may be safely obtained; therefore, it is proposed here to use the average ratio $\Delta P_a/\Delta P_s$ obtained in the test 22–25. Hence, Eq. (32) replaces Eq. (9) in the analytical model. In these equations, the model scale is included by variable h.

$$\frac{\Delta P_a}{\Delta P_s}=\frac{\rho_0 b_0 u_0^2}{gh^2(\rho_0-\rho_1)}(\text{sen}\propto_0+A^{*2})=0.0195 \tag{31}$$

$$u_0=\sqrt{\frac{0.0195gh^2(\rho_0-\rho_1)}{\rho_0 b_0(\text{sen}\propto_0+A^{*2})}} \tag{32}$$

In these test results, $\Delta P_a/\Delta P_s<1$ because the saltwater density used in this computation is the saltwater source density and h is the full height of the door and not the height between neutral plane and door sill (as deduced in the analytical model). Physically, the representative flow density is the mixture density at the door height. It was not possible during tests to assess directly this local density.

Finally, in these experiments, the time scale is $t_m/t_P=1$ and the geometric scale is $l/L=1/20$ (geometric similarity), thus, the velocity scale is $u_m/u_P=1/20$ (kinematic similarity). According to Eq. (25), which fulfils the Froude Number, the buoyancy of test 22 corresponds to the temperature difference of 372 K (T_{0P}=293K). Dynamic similarity is not fully accomplished in these experiments because the Reynolds Number in the model is ranging from 500 to 3400, while in the prototype the flow is fully turbulent.

4. Conclusions

In this paper, a set of equations has been developed, which describes the fire smoke tightness of a downward air curtain applied to an opening. Saltwater modelling was used to study the convective performance of this kind of flows and the experiments made it possible to draw the following conclusions:

1. Downward curtains may be successfully applied to avoid saltwater flow through an opening, but require exhaustion in the compartment.
2. Small scale saltwater tests show that the convective process described by the theoretical model is correct; therefore, this convective part of the model is expected to be applicable for obtaining smoke tightness of openings during fire events (adjustment of the model for fully turbulent flows will be required).
3. The test results show that the minimum jet velocity required to obtain the saltwater tightness of the opening may be given by Eq. (32).
4. Minimum saltwater exhaust flow rate from the compartment is given by Eq. (29), which agrees with Eq. (15) of the theoretical model. To obtain the minimum smoke exhaust flow rate, the term corresponding to smoke expansion due to heating must be added.

Full-size experiments, including a prototype of the air curtain and using a fire source, will be developed to verify the smoke tightness model and to adjust the model for fully turbulent flows.

Acknowledgments

This research was performed as part of a research project financially supported by *ADI – Agência de Inovação* under Grant QREN no. 23226 (Smoke Shield), through Operational Competitiveness Programme (COMPETE) as part of the National Strategic Reference Framework.

References

[1] S. Gupta, M. Pavageau, J.C. Elicer-Cortés, Cellular confinement of tunnel sections between two air curtains, Build. Environ. 42 (2007) 3352–3365.

[2] H. Sakurai, T. Hayashi, M. Shibata, K. Kanehara, Researches on air shutter for fire defence, Fire Saf. J. 2 (1979/80) 9–16.

[3] F. Cumo, S. Rossetti, G. Guidi, 3D simulation of dynamic barriers against fume and gaseous toxic substances, in: Proceedings of the 6th International Symposium on Ventilation for Contaminant Control, Helsinki, Finland, 4–7 June, 2000

[4] M. Dufresne de Virel, C. Solliec, L. Guyonnaud, Mise en sécurité contre fumées d′incendie, Rev. Face Risque 348 (1998) 13–18.

[5] M.S. Altinakar, A. Weatherill, Use of an inclined air curtain for preventing smoke propagation in a tunnel during fire emergency, in: Proceedings of the 4th International Conference on Safety in Road and Rail Tunnels, 2001

[6] F. Gugliermetti, L. Santarpia, G. Zori, Air curtain applied to fire smoke pollution control, air pollution 2003, in: Proceedings of the 11th International Conference on Modelling, Monitoring and Management of Air Pollution, Catania, Italy, September 17–19, 2003, pp. 541–549

[7] M. Sawley, B. Greveldinger, A. Drotz, Numerical flow simulation of an air curtain for road tunnel fire safety, Supercomput. Rev. 14 (2004) 3–6.

[8] L.H. Hu, J.W. Zhou, R. Huo, W. Peng, H.B. Wang, Confinement of fire-induced smoke and carbon monoxide transportation by air curtain in channels, J. Hazard. Mater. 156 (2008) 327–334.

[9] F. Felis, M. Pavageau, J.C. Elicer-Cortés, T. Dassonville, Simultaneous measurements of temperature and velocity fluctuations in a double stream-twin jet air curtain for heat confinement in case of tunnel fire, Int. Commun. Heat Mass Transf. 37 (2010) 1191–1196.

[10] Y.P. I, Y.L. Chiu, S.J. Wu, The simulation of air recirculation and fire/explosion phenomena within a semiconductor factory, J. Hazard. Mater. 163 (2009) 1040–1051.

[11] Yang-Cheng Shih, An-Shik Yang, Chang-Wei Lu, Using air curtain to control pollutant spreading for emergency management in a cleanroom, Build. Environ. 46 (2011) 1104–1114.

[12] Na Luo, Angui Li, Ran Gao, Zhenguo Tian, Wei Zhang, Sen Mei, Luman Feng, Pengfei Ma, An experiment and simulation of smoke confinement and exhaust efficiency utilizing a modified opposite double-jet air curtain, Saf. Sci. 55 (2013) 17–25.

[13] R.D. Blevins, Applied Fluid Dynamics Handbook, Van Nostrand Reinhold Company Inc, New York, USA, 1984.

[14] Carlos Viegas João, Utilização de ventilação de impulso em parques de estacionamento cobertos, Laboratório Nacional de Engenharia Civil. Série Teses e Programas de Investigação, Lisboa, 2008, p. 55.

[15] K. Steckler, H. Baum, J. Quintiere, Salt water modelling of fire induced flows in multicompartment enclosures. in: Proceedings of the Twenty-first Symposium on Combustion, 1986, 4 pp

[16] Ran Gao, Angui Li, Wenjun Lei, Yujiao Zhao, Ying Zhang, Baoshun Deng, A novel evacuation passageway formed by a breathing air supply zone combined with upward ventilation, Physica A 392 (2013) 4793–4803.

[17] Na Luo, Angui Li, Ran Gao, Wei Zhang, Zhenguo Tian, An experiment and simulation of smoke confinement utilizing an air curtain, Saf. Sci. 59 (2013) 10–18.